From pixels to percepts: Highly robust perception and exploration using deep learning and an optical biomimetic tactile sensor

Nathan F. Lepora*, Alex Church, Conrad De Kerckhove, Raia Hadsell, John Lloyd*

***Abstract*— Deep learning has the potential to have the impact on robot touch that it has had on robot vision. Optical tactile sensors act as a bridge between the subjects by allowing techniques from vision to be applied to touch. In this paper, we apply deep learning to an optical biomimetic tactile sensor, the TacTip, which images an array of 3D pins inside its sensing surface analogous to structures within human skin. Our main result is that the application of a deep CNN can give robust exploration and perception in tasks beyond which the model was trained. We demonstrate the accurate exploration of various objects, from tapping around curved shapes to continuous sliding exploration around compliant or irregular objects (e.g. a banana), using a single basic training set collected from tapping on a disk. This robustness follows from using techniques to encourage generalization beyond the task a model is trained, such as over-regularizing the network architecture. Such methods seem appropriate for robot touch because of the complexities underlying tactile sensation and interaction.**

I. INTRODUCTION

Robot touch is different from robot vision: to touch, an agent must physically interact with its environment, which constrains the form and function of its tactile sensors (for example, to be robust, compliant and compact). Likewise, tactile perception is different from visual perception: to perceive touch, an agent interprets the deformation of its sensing surface, which depends on the shape and mechanics of the sensor, unlike vison where the eye does change what can potentially be seen [1].

Therefore, the application of deep learning to robot touch will be different from robot vision, just as robot vision poses different research questions than computer vision [2]. Thus far, there have been relatively few studies of deep learning for tactile perception compared with the explosion of work on robot vision. Those studies have mainly considered one particular device – the Gelsight [3], an optical tactile sensor that images the shading from 3 internal RGB-colored LEDs to transduce surface deformation (and complements this with painted markers to detect shear [4]). Use of an optical tactile sensor seems an appropriate starting place for applying deep learning to touch, given the rapid progress for vision.

In this paper, we apply deep learning to an optical biomimetic tactile sensor, the TacTip [5], [6], which images an array of 3D pins inside its sensing surface (Fig. 1c). This transduction mimics that of the dermal papillae and intermediate ridges within human tactile skin. In past work, we used image-processing methods to track the pin positions [7], [8]. These pin positions were then passed to a distinct perception system, using statistical models [6]–[12], dimensionality reduction [13] or support vector machines [14]. Here we use a deep Convolutional Neural Network (CNN) for direct (end-to-end) perception from the tactile images.

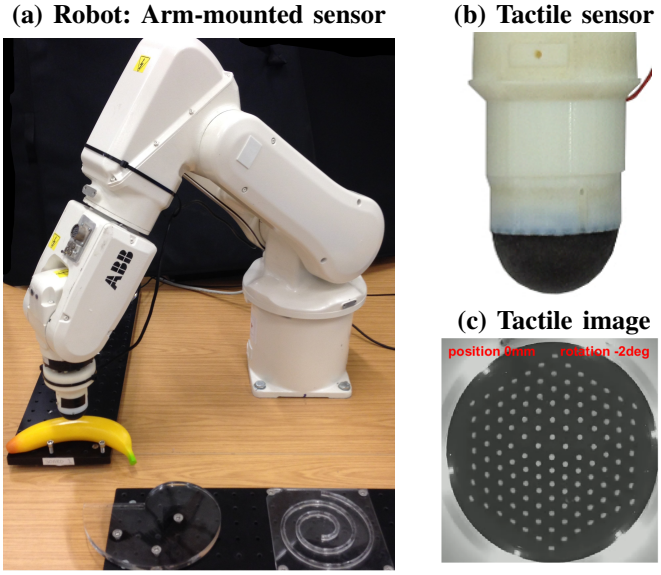

Fig. 1: Tactile robotic system, showing: (a) the arm-mounted tactile sensor next to a few objects; (b) the (TacTip) optical tactile sensor; and (c) an image from the tactile sensor.

Our main result is that a deep CNN can impart highly robust performance in tasks beyond which the model was trained. As a consequence, the tactile system can attain more complex behaviors, such as continuous sliding exploration around compliant or irregular objects, after being trained in a simpler circumstance of tapping against a disk. This robustness follows from using techniques to encourage generalization beyond the task a model is trained, such as over-regularization, data augmentation and data shifting.

II. BACKGROUND AND RELATED WORK

Initial applications of deep learning to artificial tactile perception were with taxel-based sensors. The first used a four-digit robot hand covered with 241 distributed tactile skin sensors (with another 71 motor angles, currents and force/torque readings) to recognize 20 grasped objects, using a CNN and $\sim$1000 training samples [15]. There have since been several other studies with taxel-based sensors [16]–[19].

NL and JL were supported by a Leadership Award from the Leverhulme Trust on 'A biomimetic forebrain for robot touch' (RL-2016-39).

NL, AC, CDK and JL are with the Department of Engineering Mathematics and Bristol Robotics Laboratory, University of Bristol, Bristol, U.K. Email: {n.lepora, ac14293, jl15313}@bristol.ac.uk

AC and RH are with Google DeepMind. Email: raia@google.com

* NL and JL contributed equally to this work.

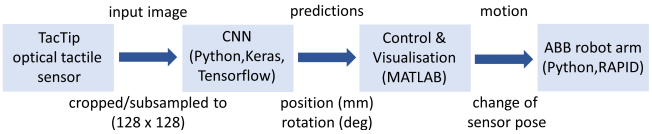

Fig. 2: System and software infrastructure, from the TacTip optical tactile sensor, to processing in Python and MATLAB, to controlling the ABB robot arm.

More recently, the Gelsight optical tactile sensor has found a natural match with deep learning, beginning with applications of CNNs to shape-independent hardness perception [20] and grasp stability [21], then considering visuo-tactile tasks for surface texture perception [22] and slip detection [23]. The original Gelsight domed form-factor has been modified to a slimmer design for better integration with a two-digit gripper [24], enabling study of tactile grasp readjustment [25] and visuo-tactile grasping [26]. The majority of these studies use a CNN trained with several thousand examples, sometimes including an LSTM layer for sequential information.

In this work, we consider tactile edge perception and object exploration. In humans, edges and vertices are the most salient local features of 3D-shape [27], [28], and are thus a key sensation for artificial tactile systems such as robot hands or prosthetics [29]. Work in robotic tactile object exploration dates back a quarter century [30]–[32], with a more recent approach adopting a control framework for tactile servoing [33]. However, these studies have relied on applying image processing techniques (*e.g.* image moments) to planar taxel arrays. For curved biomimetic sensors such as the iCub fingertip, another approach is to use a non-parametric probabilistic model of the taxel outputs [34]–[36].

The TacTip tactile sensor has also been used for edge perception and exploration, using a combination of servo control and a probabilistic model of the pin displacements [9]. After tuning the control parameters, the robot could tap around shapes such as a circle, volute and spiral. However, the trajectories [9, Figs 7-10] were not robust to parameter changes and failed when applied to sliding rather than tapping motion. Controlled sliding using touch is a challenge because the sensing surface undergoes a motion-dependent shear due to friction against the object surface. Training data will thus differ in a complex way from the sensor output during the task, which will cause supervised learning methods to fail unless shear invariance is somehow applied.

III. METHODS

A. Robotic system: Tactile sensor mounted on a robot arm

1) Tactile sensor: We use an optical biomimetic tactile sensor developed in Bristol Robotics Laboratory: the TacTip [5], [6]. The version used here is 3D-printed with a 40 mm-diameter hemispherical sensing pad (Fig. 1b) and 127 tactile pins in a triangular hexagonal lattice (Fig. 1c). Deformation of the sensing pad is imaged with an internal camera (ELP USB 1080p module; used at 640×480 pixels and ~ 30 fps). The pin deflections can accurately characterize contact location, depth, object curvature/sharpness, edge angle, shear and slip. For more details, we refer to recent studies with this tactile sensor [6]–[14], [37]–[41].

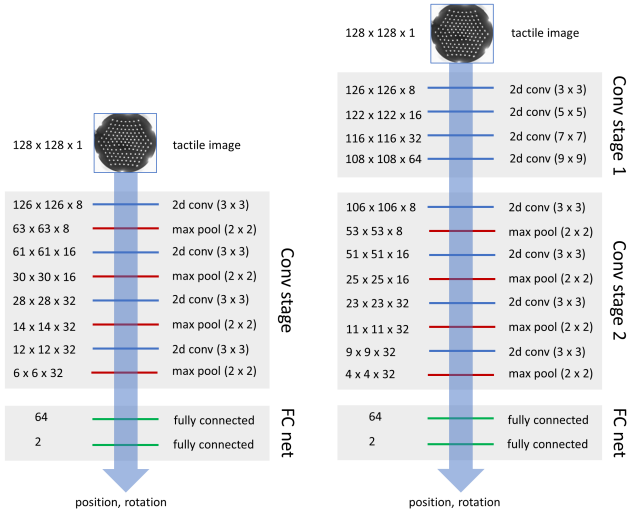

Fig. 3: The two CNN architectures used in this work. The first (a) is based on a standard CNN pattern [42] and the second (b) has an additional input stage without max pooling.

2) Robot arm mounting: The TacTip is mounted as an end-effector on a 6-DoF robot arm (IRB 120, ABB Robotics). The removable base of the TacTip is bolted onto a mounting plate attached to the rotating (wrist) section of the arm, then the other two modular components (central column and tip) are attached by bayonet fittings (Fig. 1a).

3) Software infrastructure: Our integrated sensorimotor framework has four components (Fig. 2): (1) Stacks of tactile images are collected in the OpenCV library, then preprocessed and either saved (for use in training) or passed directly to the Deep Learning system; (2) These images are first cropped and subsampled to (128×128)-pixel grey-scale images (*e.g.* Fig. 1c) and then passed to the Deep Learning system (see below) in Keras; (3) The resulting tactile percepts are passed to control and visualization software in MATLAB; (4) The change in sensor pose from the control is sent to a Python client that interfaces with a RAPID API for controlling the robot arm. Training is carried out by Titan XP GPU hosted on a Windows 10 PC. The components then run in real-time when performing the experimental tasks.

B. Deep learning system

Two types of CNN architecture are used here (Fig. 3): the first for tapping-based exploration experiments; and the second, more complex architecture, to cope with the additional challenges associated with continuous-contact exploration.

The first architecture (Fig. 3a) passes a 128×128 grey-scale image through a sequence of convolutional and max-pooling layers to generate a high-level set of tactile features. These features are then passed through a fully-connected regression network to make predictions. This configuration is based on a simple convolutional network pattern [42], which was scaled and regularized by restricting the number

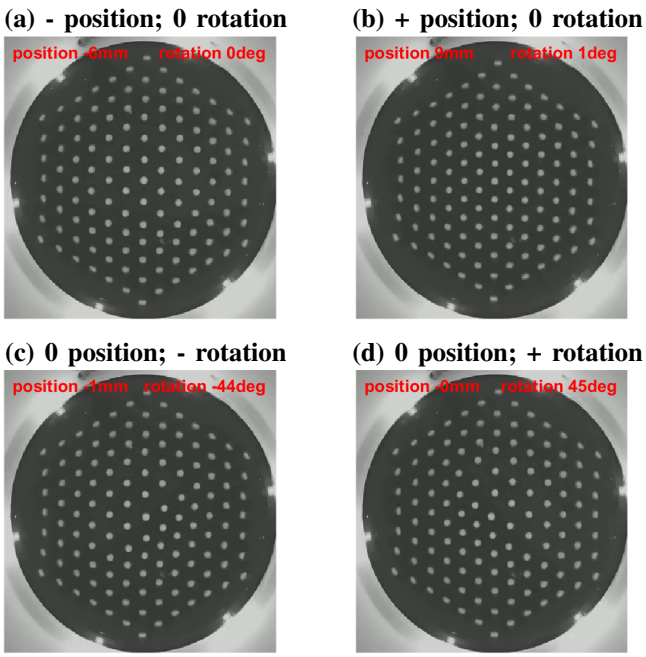

Fig. 4: Example tactile images from the deepest tapping depth at the four extremes of the range (contact radius $-6\,\mathrm{mm}$, $9\,\mathrm{mm}$ and rotation angle $-45\,\mathrm{deg}$, $+45\,\mathrm{deg}$).

of filters/ReLUs in each layer and using a dropout of 0.25 between the convolutional stage and fully-connected net.

The second architecture (Fig. 3b) was introduced to cope with the effects of non-linear shear on the sensor pin positions during continuous contact sliding motion. Under this type of motion, the pins tend to be displaced from the positions they occupy normally during tapping exploration and, consequently, their relative positions convey more useful information than their absolute positions.

Initially, we tried to encourage the original network architecture (Fig. 3a) to make use of relative pin positions by using data augmentation to introduce randomly shifted copies of the sensor images into the training data (shifting each image randomly by 0-2% in the horizontal and vertical directions on each presentation). However, this alone was not enough to achieve good performance for continuous contact exploration of objects other than the disk.

We then extended the network by adding an initial convolution stage without any max-pooling layers before the original network (Fig. 3b), which did achieve better performance. Combined with the data augmentation, this allowed the network to learn broader features over larger groups of pixels, which allows the network to capture the spatial relationship between groups of adjacent pins. Once again, we used a dropout of 0.25 between the second convolutional stage and the fully-connected net to help over-regularize the model with respect to the validation and test data.

Both network architectures were trained using the Adam optimizer, with learning rate 10^{-4} and learning rate decay 10^{-6}. Limiting the number of filters/ReLUs in each layer, using 0.25 dropout before the fully-connected net and early stopping (patience parameter 5) all helped prevent overfitting.

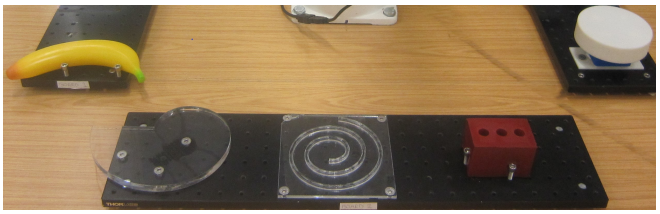

Fig. 5: The 5 objects used for tactile exploration. From right to left: a circular disk (used also for training), soft rubber brick, spiral ridge, volute lamina and plastic banana.

C. Data collection

For training, the tactile robotic system samples a local region of the edge of one object ($105\,\mathrm{mm}$ disk at 12 o'clock position) over a range of radial positions r and axial (roll) rotation angles θ, using tapping contacts on-off the edge. Here we used 2000 uniform random contacts sampled over positions $-6\,\mathrm{mm}$ to $+9\,\mathrm{mm}$ and angles $-45\,\mathrm{deg}$ to $+45\,\mathrm{deg}$, with each tap from $\sim 1.5\,\mathrm{mm}$ above the object, down $5\,\mathrm{mm}$ and taking $\sim 1\,\mathrm{sec}$ duration with ~ 30 frames. The origin $(0\,\mathrm{mm}, 0\,\mathrm{deg})$ is when the sensor tip is centred on the edge with the camera and pin lattice aligned normal to the edge (Fig. 1c). This set was split into 1600 samples for training the neural network and 400 for hyperparameter optimization.

A further dataset of 2000 contacts sampled over new random positions and angles was collected and used for evaluating perceptual performance.

There is modest scope for improving the results by fine-tuning these experiment parameters. However, trial and error (and experience with the experimental paradigm [9]) showed these to be reasonable and natural choices. The only non-obvious choice was to include a random shift between $\pm 1\,\mathrm{deg}$ of the sensor yaw/pitch in all data to provide some insensitivity to these variables. This reduced specialisation in the trained network to small but noticeable non-normal sensor alignments that otherwise biased the angle predictions.

All tactile images are cropped and subsampled to a (128×128)-pixel region containing the pins. Images sampled around the peak displacement of each tap were used to also provide some insensitivity to sensor depth in the trained network. Here we used 7 frames centred on the peak frame (measured by the RMS changes in pixel intensity from the initial frame). Example peak contacts near the four extremes of the range $(-6\,\mathrm{mm}, 0\,\mathrm{deg})$, $(+9\,\mathrm{mm}, 0\,\mathrm{deg})$ and $(0\,\mathrm{mm}, \pm 45\,\mathrm{deg})$ are shown in Fig. 4.

D. Task: Exploratory tactile servoing

Here we consider tasks in which a tactile sensor moves along a continuously-extended tactile feature such as the edge of an object, while rotating to maintain alignment with that feature. We consider this to be an exploration task because the sensor moves onto a previously unknown part of the object and tactile servoing because the sensor maintains its angle of alignment with the tactile feature.

These tasks are performed on a range of objects (Fig. 5) chosen for a variety of shapes and material properties: a

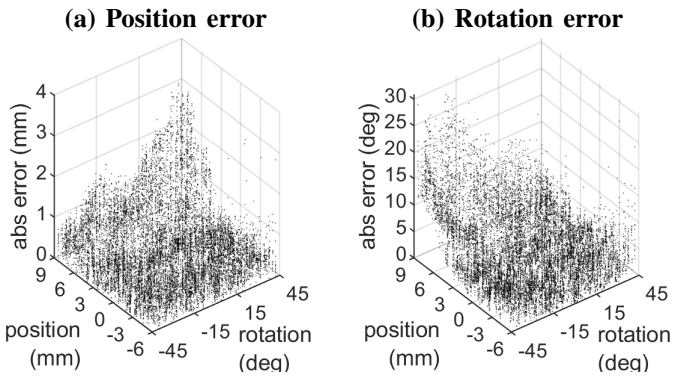

Fig. 6: Radial position and angular rotation prediction errors for the first CNN architecture (Fig. 3a) applied to 2000 random taps of 7 frames each. Absolute errors are shown.

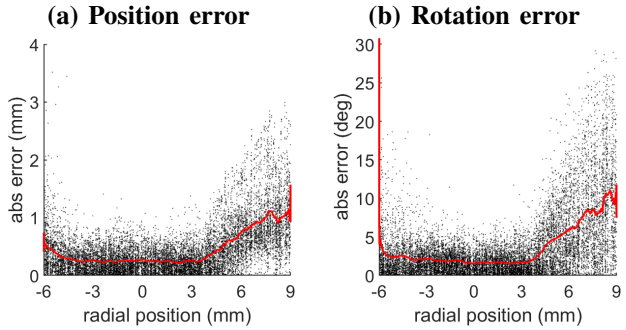

Fig. 7: CNN prediction errors from Fig. 6 over radial position only. The red curve is a mean calculated from a 500-point (1/28 of the range) moving-average filter.

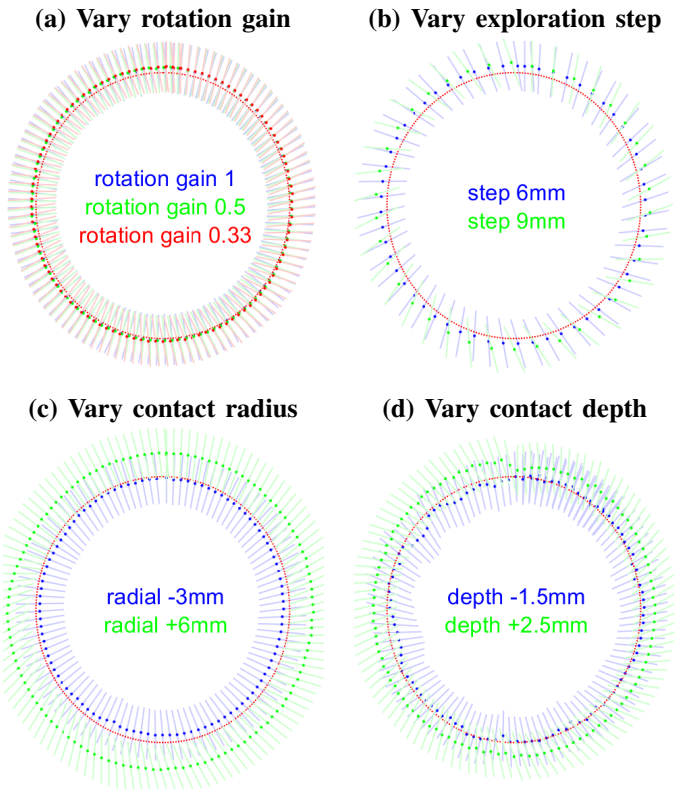

Fig. 8: Robustness of tapping exploration around the disk. The changes are relative to the default parameters given in Sec. IIID (rotation gain 0.5, step 3 mm, radius $r_{\text{fix}} = 0$ mm).

105 mm-diameter circular disk (3D-printed in ABS plastic), a lamina volute with radii of curvature $30, 40, 50, 60$ mm in 90 deg segments (laser-cut from acrylic plastic), a 5 mm-wide ridge in a volute spiral with radii of curvature $20, 30, 40, 50, 60$ mm in 180 deg segments (also laser-cut) and two objects from the YCB object set [43], one chosen to be compliant (a soft rubber brick) and the other to be irregular (a plastic banana). Note that only the circular disk is used to gather training data (at the 12 o'clock position).

A simple controller takes the perceptual predictions (r, θ) for the sensor pose relative to the edge, with output action having three components [9]: (i) a radial move Δr along the (predicted) normal to the edge towards a fixed position r_{fix}; (ii) an exploratory move Δe along the (predicted) tangent to the edge at angle θ; and (iii) reorienting the sensor $\Delta\theta$ towards a fixed angle θ_{fix}. This is a proportional controller

$$\Delta r = g_r \left(r - r_{\text{fix}}\right), \quad \Delta\theta = g_\theta \left(\theta - \theta_{\text{fix}}\right), \qquad (1)$$

with gains (g_r, g_θ). Defaults are $(g_r, g_\theta) = (1, 0.5)$, $\Delta e = 3$ mm and $(r_{\text{fix}}, \theta_{\text{fix}}) = (0\,\text{mm}, 0\,\text{deg})$ from ref. [9]. During the task, the tactile robot begins at this fixed relative pose and seeks to maintain it while moving around the object edge.

IV. RESULTS

A. End-to-end perception from tactile images

In a major departure from recent work with the TacTip optical biomimetic sensor, here we predict the percepts directly from tactile images with a deep CNN. Prior work with this sensor has used specialised preprocessing to detect then track the pin positions [6]–[14], [37]–[41]. Here, this preprocessing is subsumed into the trained neural network.

We report this performance for the first CNN architecture (Fig. 3a). During our preliminary investigations, we found that networks with more filters/ReLUs in each layer and less regularization achieved better performance on the validation and test data collected at the same point on the disk as where the training data was collected. However, they failed to generalize well to other regions of the disk or to other objects. Over-regularizing the network beyond the point required for good generalization on the test data helped solve this problem and produced models that perform well on a broader range of tapping-based exploration tasks.

The overall perceptual performance is then most accurate near the central positions for all rotations (Fig. 6; 14000 samples shown). In this region (-3 mm to 3 mm), errors are generally less than 1 mm and 5 deg. Overall, the contacts are less informative as they move away from the edge (9 mm into free space; -6 mm onto the disk), consistent with the edge being no longer visible in those tactile images (*e.g.* Figs 4a,b). Considering only the dependence on position (Fig. 7), the mean absolute errors are ~ 0.3 mm and ~ 2 deg in the central region where perception is most accurate (red curve). These accuracies are appropriate for the exploration task considered in the following sections.

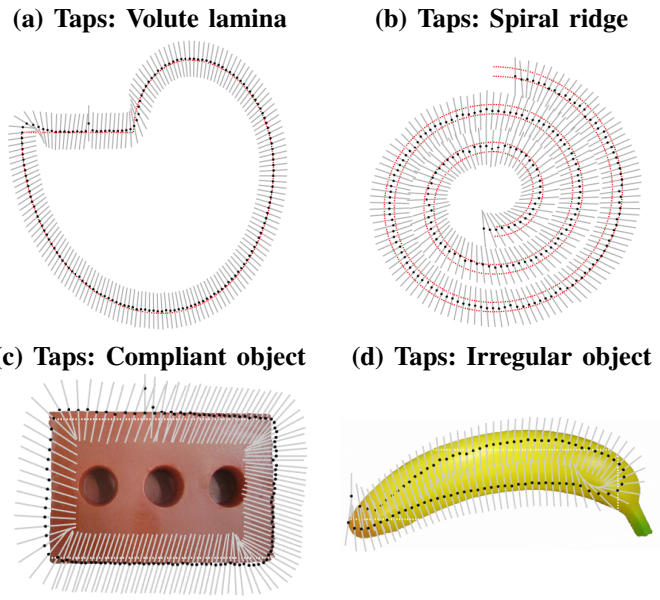

Fig. 9: Robustness of tapping exploration to non-uniform object shapes (using training data from tapping on the disk).

B. Robust exploratory tactile servoing around a disk

The deep CNN is now applied to tactile exploration around a uniform disk, using a tapping motion like that for the training data. Servo control (Eq. 1) maintains a similar pose with the edge while moving around the disk, using the predicted edge angle and position.

The trajectories from tactile exploration are near-perfect circles around the disk under a range of conditions (Fig. 8; Table I). Reducing the angle gain in the controller from 1 leaves the trajectory within 1 mm of the edge, but biases the sensor angle from 4 deg to 17 deg (Fig. 8a; $g_\theta = 0.33, 0.5, 1$). A smaller gain can improve stability on more complex tasks, so we generally use $g_\theta = 0.5$ and accept a bias of 9 deg. Increasing the exploration step size from 3 mm keeps the trajectory within 2 mm of the edge, but amplifies the angle bias (Fig. 8b; $\Delta e = 6, 9$ mm). Likewise, a radius inside or outside the edge keeps a circular trajectory but with an angle bias of 11 deg or 29 deg (Fig. 8c; $r_{\text{fix}} = -3, +6$ mm).

The circular trajectories are also robust to changing the tapping depth (Fig. 8d, depth change $\Delta = -1.5, +2.5$ mm), from shallow taps (blue points; 3 mm above, down 5 mm) to deep taps (green points; -1 mm above, down 5 mm). However, shallow taps advanced the rotation angle by 11 deg, and deep taps lagging the angle by 29 deg. This bias is because the training data is at a different depth from the data during the task. Although the CNN is most accurate for taps at the training depth, its performance has declined gracefully to still complete the exploration task.

These results are a major improvement over those obtained in a previous study on the same task with a probabilistic model of pin displacements [9] (comparison in Table I), which failed to complete the task in many circumstances.

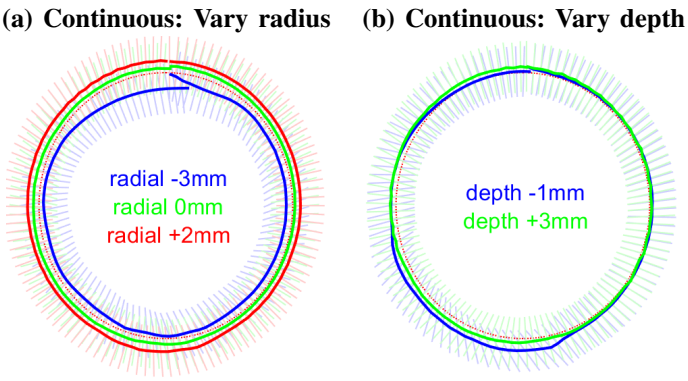

Fig. 10: Robustness of sliding exploration around the disk (using training data from tapping on the disk).

C. Robustness to non-uniform object shapes

To demonstrate further robustness, the task is extended to two fabricated planar shapes chosen to have non-uniform curvature (a volute lamina and a spiral ridge) and two household objects from the YCB object set [43]: one compliant (a soft rubber brick) and one irregular (a plastic banana). Tactile exploration of objects demonstrates generalization to novel edges that differ from the disk edge used for training.

For the volute lamina and spiral ridge, the exploration trajectories match the object shapes (Figs 9a,b). When the radius of curvature is close to that of the disk, the sensor angle aligns to the edge normal. For smaller or larger curvatures, there is bias in the sensor angle (advancing for smaller and lagging for higher) while the radial position remains accurate. We note that these results hold on the spiral even though its surface (a 5 mm-wide ridge) is very different from the disk edge used for training.

For the compliant and irregular objects, the exploration also completes (Figs 9c,d). The rubber brick deforms visibly under the tapping motion, yet the position perception remained accurate. The banana had slight ridges between the segments of skin and also varied in height by a few millimetres, yet the exploration trajectories followed these ridges and turned when the depth dropped at the stalk.

experiment	parameter variation	probabilistic model [9]	deep CNN
tapping contact (Fig. 8a)	$g_\theta = 1.0$	fail	1 mm, 4 deg
	$g_\theta = 0.5$	3 mm, 10 deg	1 mm, 9 deg
	$g_\theta = 0.33$	3 mm, 19 deg	1 mm,17 deg
tapping contact (Fig. 8b)	$\Delta e = 6$mm	8 mm, 24 deg	1 mm, 23 deg
	$\Delta e = 9$mm	fail	2 mm, 38 deg
tapping contact (Fig. 8c)	$r_{\text{fix}} = -3$mm	10 mm, 23 deg	1 mm, 12 deg
	$r_{\text{fix}} = +6$mm	fail	6 mm, 23 deg
tapping contact (Fig. 8d)	$\Delta = -1.5$mm	fail	1 mm, 12 deg
	$\Delta = +2.5$mm	fail	3 mm, 29 deg
sliding contact (Fig. 10a)	$g_\theta = 1.0$	fail	1 mm, 4 deg
	$g_\theta = 0.5$	fail	1 mm, 9 deg
	$g_\theta = 0.33$	fail	1 mm, 17 deg
sliding contact (Fig. 10b)	$\Delta e = 6$mm	fail	1 mm, 23 deg
	$\Delta e = 9$mm	fail	2 mm, 38 deg

Table I. Accuracy of exploration around the disk, showing the mean absolute errors of radial position and rotation angle for the trajectories in Figs 8,10. A comparison is shown with the original probabilistic model [9] for each experiment.

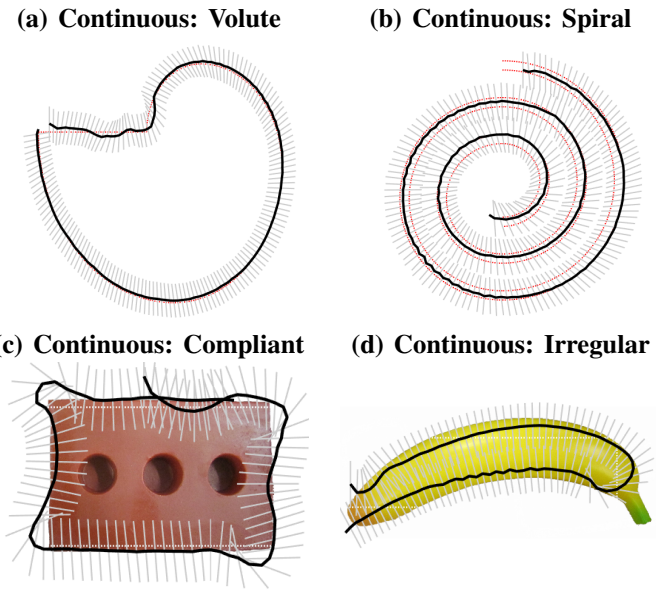

Fig. 11: Robustness of sliding exploration to non-uniform object shape (using training data from tapping on the disk).

D. Robustness to continuous sliding contact

A far more demanding test of robustness is to explore object shape with a continuous sliding motion while still using the same training data from tapping the disk edge. Hence, we repeat the above experiments, dropping the sensor $3\,\mathrm{mm}$ ($1.5\,\mathrm{mm}$ into the object) and collecting data between the exploratory movements ($\sim 0.15\,\mathrm{sec}$ duration; ~ 5 frames). For these experiments, the second CNN architecture (Fig. 3a) was uses, which has an initial convolution stage without any max-pooling layers to help generalize over tactile features.

The circular trajectories are robust to changes in contact radius (Fig. 10a; $r_{\mathrm{fix}} = -3, +2\,\mathrm{mm}$) and depth (Fig. 10b; $-1\,\mathrm{mm}$ shallower, $+3\,\mathrm{mm}$ deeper). The range of contact depths was the same ($4\,\mathrm{mm}$) for taps and sliding, although we did not try greater depths because of concerns about damaging the sensor (which was kept the same for all experiments). The angle bias improved to $4\,\mathrm{deg}$ with greater contact depth, which is actually the joint best overall trajectory (equal with the gain $g_\theta = 1$ tapping trajectory).

For the volute and spiral, the trajectories again successfully explored the objects (Figs 11a,b), with very similar trajectories as the tapping exploration (*c.f.* Figs 9a,b). There is a wobble on the starting straight segment of the volute, which appears due to an initial irregularity in shear direction that is later attenuated by the steadier motion. Otherwise, the trajectory follows the volute, with some bias in rotation angle when the volute curvature differs from that of the disk.

Finally, the compliant and irregular objects were also successfully explored (Figs 11c,d). The compliance and shear affect performance when turning the corners of the rubber brick compared with the tapping motion, with little difference along the straight edges (*c.f.* Figs 9c,11c). The irregularly-shaped plastic banana has an almost identical trajectory for both tapping and sliding exploration (*c.f.* Figs 9d,11d), tracing the slight ridge between sections of the banana skin.

V. Discussion

This work is the first application of deep learning to an optical biomimetic tactile sensor and the first application to an object exploration task. Our main result is that a deep CNN can impart highly robust performance in tasks beyond which the model was trained, such as continuous sliding exploration around compliant or irregular objects (*e.g.* a banana) after being trained by tapping on part of a disk.

The tasks progressed from: (i) testing on the same region of the disk as the training data; (ii) circling the disk under variations in tap depth and servo control; (iii) exploring around volute and spiral objects with changing edge curvature; (iv) exploring around compliant and irregular objects; and (v) attaining all of these with a sliding rather than tapping contact. The challenge of this generalization is that the task data becomes progressively less like the data on which the model is trained.

Here we used two techniques to encourage generalization beyond the task a model is trained on. The first technique was to anticipate the nuisance variables whose effect should be marginalised out and then either modify the data collection (e.g. training over shifts in yaw/pitch) or augment the data set with artificially generated data (randomly shifting frames by up to 2%). The second technique was to over-regularize the architecture to avoid specialization to the training task; this may be because it encourages the development of simpler features throughout the network. In both cases, we are introducing inductive bias into the model to improve performance in situations different from its training. This is necessary because generalizing beyond the task a model is trained on cannot be reliably achieved by trying to validate on data from the original task

This manner of task generalization seems particularly appropriate for robot touch. Tactile sensors function by measuring the deformation of their surface. Hence, any interaction of the sensor with an object will affect the sensation, which is a generic situation for cutaneous tactile sensing based on human fingertips, whether they be integrated in grippers/manipulators or used as probes. Unless the circumstances are very restricted, the tactile data during a task can differ in complex ways from those during training. For example, sliding causes a friction-dependent shear (and maybe slip) of the sensing surface that depends on the motion velocity, contact force and recent history of the interaction.

Achieving this task generalization may help attain more general and robust tactile control than has thus far been reached. For example, here we generalized to a fairly complex behaviour (feeling around the segments of a banana) from a basic training regime of tapping at a single location on a disk. It would be interesting to see what this approach can achieve has when applied to more degrees of freedom, such as 3D interactions or multi-fingered manipulators.

Acknowledgements: We thank members of the BRL Tactile Robotics group for help: Ben Ward-Cherrier, Nick Pestell, Luke Cramphorn, Kirsty Aquilina, Pernilla Craig and Jasper James. We thank NVIDIA for donation of a Titan XP GPU.

REFERENCES

[1] V. Hayward. Is there a 'plenhaptic' function? **Philosophical Transactions of the Royal Society B: Biological Sciences*, 366(1581):3115–3122, 2011.

[2] N Sünderhauf, O Brock, W Scheirer, R Hadsell, D Fox, J Leitner, B Upcroft, P Abbeel, W Burgard, M Milford, and P Corke. The limits and potentials of deep learning for robotics. *The International Journal of Robotics Research*, 37(4-5):405–420, apr 2018.

[3] W Yuan, S Dong, and E Adelson. GelSight: High-Resolution Robot Tactile Sensors for Estimating Geometry and Force. *Sensors*, 17(12):2762, 2017.

[4] Wenzhen Yuan, Rui Li, Mandayam A Srinivasan, and Edward H Adelson. Measurement of shear and slip with a GelSight tactile sensor. *2015 IEEE International Conference on Robotics and Automation (ICRA)*, 2015-June:304–311, 2015.

[5] C. Chorley, C. Melhuish, T. Pipe, and J. Rossiter. Development of a Tactile Sensor Based on Biologically Inspired Edge Encoding. In *International Conference on Advanced Robotics (ICAR)*, pages 1–6, 2009.

[6] B. Ward-Cherrier, N. Pestell, L. Cramphorn, B. Winstone, M. E. Giannaccini, J. Rossiter, and N. F. Lepora. The TacTip Family: Soft Optical Tactile Sensors with 3D-Printed Biomimetic Morphologies. *Soft Robotics*, pages 1–13, 2018.

[7] N. Lepora and B. Ward-Cherrier. Superresolution with an optical tactile sensor. In *IEEE/RSJ International Conference on Intelligent Robots and Systems (IROS)*, pages 2686–2691, 2015.

[8] N. Lepora. Biomimetic Active Touch with Fingertips and Whiskers. *IEEE Transactions on Haptics*, 9(2), 2016.

[9] N. Lepora, K. Aquilina, and L. Cramphorn. Exploratory Tactile Servoing with Active Touch. *IEEE Robotics and Automation Letters*, 2(2):1156–1163, 2017.

[10] Benjamin Ward-Cherrier, Luke Cramphorn, and Nathan F. Lepora. Exploiting Sensor Symmetry for Generalized Tactile Perception in Biomimetic Touch. *IEEE Robotics and Automation Letters*, 2(2):1218–1225, 2017.

[11] L. Cramphorn, B. Ward-Cherrier, and N. Lepora. Addition of a Biomimetic Fingerprint on an Artificial Fingertip Enhances Tactile Spatial Acuity. *IEEE Robotics and Automation Letters*, 2(3):1336–1343, 2017.

[12] L. Cramphorn, B. Ward-Cherrier, and N.F. Lepora. Tactile manipulation with biomimetic active touch. In *Proceedings - IEEE International Conference on Robotics and Automation*, volume 2016-June, 2016.

[13] K Aquilina, D Barton, and N Lepora. Principal Components of Touch. *IEEE International Conference on Robotics and Automation (ICRA)*, 2018.

[14] J James, N Pestell, and N Lepora. Slip Detection with an Optical Tactile Sensor. *IEEE International Conference on Robotics and Automation (ICRA)*, 2018.

[15] A Schmitz, Y Bansho, K Noda, H Iwata, T Ogata, and S Sugano. Tactile object recognition using deep learning and dropout. *2014 IEEE-RAS International Conference on Humanoid Robots*, pages 1044–1050, 2014.

[16] L Cao, R Kotagiri, F Sun, H Li, W Huang, Z Maung, and Maung Aye. Efficient Spatio-Temporal Tactile Object Recognition with Randomized Tiling Convolutional Networks in a Hierarchical Fusion Strategy. *Proceedings of the Thirtieth AAAI Conference on Artificial Intelligence.*, 2015.

[17] M Meier, F Patzelt, R Haschke, and H Ritter. Tactile Convolutional Networks for Online Slip and Rotation Detection. *icann*, 2016.

[18] S Baishya and B Bäuml. Robust material classification with a tactile skin using deep learning. *IEEE International Conference on Intelligent Robots and Systems*, 2016-Novem:8–15, 2016.

[19] J Kwiatkowski, D Cockburn, and V Duchaine. Grasp stability assessment through the fusion of proprioception and tactile signals using convolutional neural networks. In *2017 IEEE/RSJ International Conference on Intelligent Robots and Systems (IROS)*, pages 286–292. IEEE, sep 2017.

[20] W Yuan, C Zhu, A Owens, M Srinivasan, and E Adelson. Shape-independent hardness estimation using deep learning and a GelSight tactile sensor. In *2017 IEEE International Conference on Robotics and Automation (ICRA)*, pages 951–958. IEEE, may 2017.

[21] R Calandra, A Owens, M Upadhyaya, W Yuan, J Lin, E Adelson, and Sergey Levine. The Feeling of Success: Does Touch Sensing Help Predict Grasp Outcomes? *CoRL 2017*, (CoRL):1–10, 2017.

[22] W Yuan, S Wang, S Dong, and E Adelson. Connecting Look and Feel: Associating the visual and tactile properties of physical materials. *Proceedings - 30th IEEE Conference on Computer Vision and Pattern Recognition, CVPR 2017*, 2017-Janua:4494–4502, 2017.

[23] L Jianhua, D Siyuan, and E Adelson. Slip Detection with Combined Tactile and Visual Information. 2018.

[24] E Donlon, S Dong, M Liu, J Li, E Adelson, and A Rodriguez. Gel Slim : A High-Resolution, Compact, Robust, and Calibrated Tactile-sensing Finger. *IEEE Robotics and Automation Letters*, 2018.

[25] F Hogan, M Bauza, O Canal, E Donlon, and A Rodriguez. Tactile Regrasp : Grasp Adjustments via Simulated Tactile Transformations. 2018.

[26] Roberto Calandra, Andrew Owens, Dinesh Jayaraman, Justin Lin, and Wenzhen Yuan. More Than a Feeling : Learning to Grasp and Regrasp using Vision and Touch. *IEEE Robotics and Automation Letters*, (1):1–8, 2018.

[27] M Plaisier, W Tiest, and A Kappers. Salient features in 3-D haptic shape perception. *Attention, perception & psychophysics*, 71(2):421–430, 2009.

[28] Susan J. Lederman and Roberta L. Klatzky. Relative Availability of Surface and Object Properties during Early Haptic Processing. *Journal of Experimental Psychology: Human Perception and Performance*, 23(6):1680–1707, 1997.

[29] R Ponce Wong, R Hellman, and V Santos. Spatial asymmetry in tactile sensor skin deformation aids perception of edge orientation during haptic exploration. *IEEE transactions on haptics*, 7(2):191–202, 2013.

[30] A Berger. On Using a Tactile Sensor for Real-Time Feature Extraction. *Master's thesis, Carnegie-Mellon University.*, 1988.

[31] A Berger and P Khosla. Using Tactile Data for Real-Time Feedback. *The International Journal of Robotics Research*, 10(2):88–102, 1991.

[32] N. Chen, H. Zhang, and R. Rink. Edge tracking using tactile servo. *Proceedings 1995 IEEE/RSJ International Conference on Intelligent Robots and Systems. Human Robot Interaction and Cooperative Robots*, 2:84–89, 1995.

[33] Q Li, C Sch, R Haschke, and H Ritter. A control framework for tactile servoing. *Rss2013*, (June), 2013.

[34] U. Martinez-Hernandez, G. Metta, T.J. Dodd, T.J. Prescott, L. Natale, and N.F. Lepora. Active contour following to explore object shape with robot touch. In *2013 World Haptics Conference, WHC 2013*, 2013.

[35] U. Martinez-Hernandez, T. Dodd, T.J. Prescott, and N.F. Lepora. Active Bayesian perception for angle and position discrimination with a biomimetic fingertip. In *IEEE International Conference on Intelligent Robots and Systems*, 2013.

[36] U Martinez-Hernandez, T Dodd, M Evans, T Prescott, and N Lepora. Active sensorimotor control for tactile exploration. *Robotics and Autonomous Systems*, 87:15–27, jan 2017.

[37] B. Ward-Cherrier, N. Rojas, and N. Lepora. Model-Free Precise in-Hand Manipulation with a 3D-Printed Tactile Gripper. *IEEE Robotics and Automation Letters*, 2(4):2056–2063, 2017.

[38] B. Ward-Cherrier, L. Cramphorn, and N.F. Lepora. Tactile Manipulation with a TacThumb Integrated on the Open-Hand M2 Gripper. *IEEE Robotics and Automation Letters*, 1(1), 2016.

[39] L. Cramphorn, J. Lloyd, and N. Lepora. Voronoi Features for Tactile Sensing: Direct Inference of Pressure, Shear and Contact Locations. *IEEE International Conf on Robotics and Automation (ICRA)*, 2018.

[40] Nathan F Lepora and Benjamin Ward-cherrier. Tactile Quality Control with Biomimetic Active Touch. *IEEE Robotics and Automation Letters*, 1(2):646–652, 2016.

[41] Nicholas Pestell, John Lloyd, Jonathan Rossiter, and Nathan Lepora. Dual-Modal Tactile Perception and Exploration. *IEEE Robotics and Automation Letters*, pages 1–8, 2018.

[42] I Goodfellow, Y Bengio, and A Courville. *Deep Learning*. MIT Press, 2016.

[43] B Calli, A Wallsman, A Singfh, and S Srinivasa. Benchmarking in Manipulation Research. *IEEE Robotics and Automation Magazine*, (September):36–52, 2015.